2019-04-23

A mixed reality framework for surgical navigation: approach and preliminary results

Shravan Murlidaran
Worcester Polytechnic Institute

A mixed reality framework for surgical navigation: approach and preliminary results

by

Shravan Murlidaran

A dissertation submitted in partial satisfaction of the
requirements for the degree of
Master's

in

Robotics Engineering

in the

Graduate Division

of the

Worcester Polytechnic Institute

Committee in charge:

Professor Loris Fichera , Chair
Professor Dmitry Korkin
Professor Gregory Fischer

Spring 2019

The dissertation of Shravan Murlidaran, titled A mixed reality framework for surgical navigation: approach and preliminary results, is approved:

Chair _____ Date _____

_____ Date _____

_____ Date _____

Worcester Polytechnic Institute

Abstract

A mixed reality framework for surgical navigation: approach and preliminary results

by

Shravan Murlidaran

Master's in Robotics Engineering

Worcester Polytechnic Institute

The overarching purpose of this research is to understand whether Mixed Reality can enhance a surgeons manipulations skills during minimally invasive procedures. Minimally-invasive surgery (MIS) utilizes small cuts in the skin - or sometimes natural orifices - to deploy instruments inside a patients body, while a live video feed of the surgical site is provided by an endoscopic camera and displayed on a screen. MIS is associated with many benefits: small scars, less pain and shorter hospitalization time as compared to traditional open surgery. However, these benefits come at a cost: because surgeons have to work by looking at a monitor, and not down on their own hands, MIS disrupts their eye-hand coordination and makes even simple surgical maneuvers challenging to perform. In this study, we wish to use Mixed Reality technology to superimpose anatomical models over the surgical site and explore if it can be used to mitigate this problem.

Acknowledgements

I would like to acknowledge Professor Loris Fichera for giving me the opportunity to work on this thesis and his invaluable support and advise throughout this work. I would also like to thank Professor Dmitry Korkin and Professor Gregory Fischer for being on my thesis advisory committee and providing me with their insights on the project. Furthermore, I would like to thank all the lab members of Cognitive Medical Technology (COMET) Robotics Research Lab for helping me at various stages during the project. This research was performed using resources at Worcester Polytechnic Institute. Lastly, I would like to thank my parents, my sister and all of my family for supporting me and motivating me throughout my Masters and to my friends for always being there for me.

List of Acronyms

1. **AR** : Augmented Reality
2. **CT** : Computed Tomography
3. **EM** : Electro-Magnetic
4. **FLE** : Fiducial Localization Error
5. **FPS** : Frames Per Second
6. **FRE** : Fiducial Registration Error
7. **HMD** : Head Mounted Device
8. **IGS** : Image Guided Surgeries
9. **IPD** : Inter-Pupillary Distance
10. **LOS** : Line Of Sight
11. **MIS** : Minimally Invasive Surgeries
12. **MR** : Mixed Reality
13. **MRI** : Magnetic Resonance Imaging
14. **NDI** : Northern Digital Inc.
15. **OR** : Operating Room

16. **PD** : Percentage Difference
17. **RMS** : Root Mean Squared
18. **SCU** : Sensor Control Unit
19. **SIU** : Sensor Interface Unit
20. **SLAM**: Simultaneous Localization And Mapping
21. **TCP** : Transmission Control Protocol
22. **TRE** : Target Registration Error
23. **UDP** : User Datagram Protocol
24. **VC** : Virtuality Continuum
25. **WRF** : World Reference Frame

Contents

List of Figures

Chapter 1

Introduction

Minimally invasive surgery (MIS) denotes a class of surgical procedures wherein instruments are deployed inside a patient's body through either small cuts in the skin - or natural orifices, while a live video feed of the surgical site is provided by an endoscopic camera and displayed on a screen. MIS has shown tremendous success as an alternative to traditional open surgeries in many cases because of smaller cuts which implies lower post-operative pain which in turn

Figure 1.1: A simple laparoscopic navigational task performed by a user in our study.

minimize the morbidity due to immobility and leads to faster recovery[10, 24].

The benefits of MIS comes at a cost. Figure 1.1 shows a user performing a simple laparoscopic (MIS) navigational task using the experimental setup developed in this thesis. The user has to work by looking at a monitor, and not down on his own hands. This setup disrupts the users' hand-eye coordination and makes even simple surgical maneuvers challenging to perform. Prior studies indicate that longer training periods are required for surgeons in the early stages of a surgeon's overall experience with MIS[10].

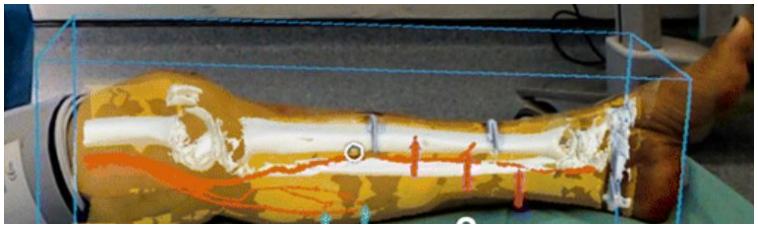

Figure 1.2: Mixed Reality technology in operating room. Image taken from [21].

Recent years have seen the usage of Mixed Reality technology which could potentially be used to superimpose the anatomical and tracking data from IGS onto the patient [6, 23, 7, 8, 18, 12]. Figure 1.2 provides an example of such a display in the operating room. Intuitively, such displays should restore the hand-eye coordination of the surgeons and improve their performance and lessen their training time. The goal of this thesis is to develop our own Mixed Reality Image Guidance system to explore if Mixed Reality has the potential to enhance surgeons' hand-eye coordination during MIS.

1.1 Contributions

The following were the contributions made as part of this thesis.

- **Design of a Mixed Reality Image Guidance Application**: A Mixed Reality Image Guidance application was developed using a Mixed Reality head-mounted display, the Microsoft HoloLens, and an electromagnetic tracker.

- **Implementation of an experimental setup where simple surgical tasks can be executed with the help of Mixed Reality**: This application was used to create an experimental setup to test surgeons' performance with HoloLens.
- **Investigation of user performance during a mock surgical task using Mixed Reality**: The experimental setup was used to conduct a study with five users and preliminary data were collected and analyzed to understand whether Mixed Reality can restore hand-eye coordination.

Chapter 2

Background

This chapter introduces the fundamental concept and technical terms used in Mixed Reality and Image-guided surgery to provide a firm understanding for readers from all backgrounds. We further discuss the contemporary research that uses Mixed Reality technology to assist Image Guided surgery to provide a foundation for our work.

2.1 Mixed Reality (MR)

A Mixed Reality environment is a blend of physical and digital worlds. It consists of virtual (any object that exists in essence or effect, but not formally or actually (hologram)) and real objects (any object that has an actual objective existence) present in the same visual display environment like Monitors, Head Mounted Devices, etc. With the advancements in computational and environment sensing capabilities, Mixed Reality is considered to be the next evolution in human, computer and environment interactions[3].

2.1.1 The Mixed Reality Spectrum (Virtuality continuum)

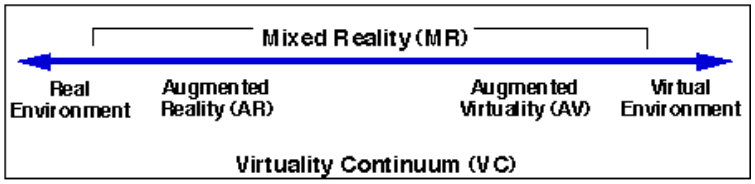

Figure 2.1: Simplified representation of a"virtuality continuum". Image reproduced from [19].

Milgram et al.[19] introduces the concept of a "virtuality continuum" as the mixture of a spectrum of real and virtual objects presented in any particular display situation, as illustrated in Figure 2.1, where real environments, are shown at one end of the continuum, and virtual environments, at the opposite extremum. Virtuality Continuum gives us a basic understanding of the breadth of displays that fall under Mixed Reality. For instance, displays that fall at the left side of the spectrum defines environments consisting solely of real objects (Figure 2.2a), and includes for example what is observed via a conventional video display of a real-world scene. An additional example includes direct viewing of the same real scene, but not via any particular electronic display system. The latter case, at the right, defines environments consisting solely of virtual objects, an example of which would be a conventional computer graphic simulation, immersive headsets (Oculus rift), etc. (Figure 2.2c). Therefore, The a Mixed Reality environment is one in which real world and virtual world objects are presented together within a single display, that is, anywhere between the extrema of the virtuality continuum (Figure 2.2b). For a more detailed classification refer [19].

(a) (b) (c)

Figure 2.2: Types of Displays. (a) Real World Display (b) Mixed World Display. (c) Virtual World Display. Source: Microsoft Mixed Reality Docs.

This definition also gives a measure to define the type of device/application that will be suitable for our purpose. As mentioned earlier, superimposing 3D anatomical data over the surgical site would require a good understanding of the environment, and a display that provides a realistic and high definition view of the 3d anatomical model (virtual object) superimposed over the surgical site (real object) whose position, orientation and scale is invariant to the surgeons head movement. This implies we need devices that can seamlessly blend real and digital world.

With the availability of HoloLens in our lab which is one of the devices that can suit our needs, we decided to conduct our study with HoloLens as our Mixed Reality device. Long Qian et al.[22] have identied HoloLens to have the highest performance among Optical See Through (OST) devices for visualization of medical information. Figure 2.3 shows the hardware characteristics of the devices used in this study. HoloLens has also been extensively studied by various groups on its capabilities [25, 14] and usefulness in medical applications [5, 8, 23].

	Moverio BT-200	ODG R-7	Microsoft HoloLens
Processor	1.2 GHz dual core	2.7 GHz quad core	1 GHz CPU, HPU
Memory	1 GB RAM	3 GB RAM	2 GB RAM
Optical design	Projector-based with LCD	Projector-based	Holographic waveguide
Screen	Dual 960 × 540	Dual 1280 × 720	2.3M holographic light points, 2.5 k/rad
Field of view	23° Diagonal	30° Diagonal	About 35°
Video resolution	640 × 480	1280 × 720	1280 × 720
OS	Android	ReticleOS (Android)	Windows Holographic
Weight	88 g	125 g	579 g
Fixture	Ear hook	Overhead strap, ear hook	Overhead strap

Figure 2.3: Overview of OST HMDs characteristics studied in[22]. Image reproduced from [22].

Optical See Through (OST) Head Mounted Devices (HMD) such as the HoloLens, Magic Leap, Moverio BT-200, etc. are some of the devices that are prime candidates for our purpose. Out of these, We conducted our study using HoloLens as our Mixed Reality device.

2.2 HoloLens

HoloLens is an Optical See-through, Head Mounted Holographic Computer developed and Manufactured by Microsoft. It runs the Windows 10 Operating System and uses the Windows Mixed Reality platform to develop applications.

2.2.1 System Overview

The HoloLens has Holographic waveguides within the display. It is a technology that allows a unidirectional wave of light to be guided through a lens or plate[4]. This technology is used for projecting virtual objects on to the real world via the see-through display. It has 1 IMU, 4 environment understanding cameras (2 on each side, See Figure 2.4), 1 2MP photo/HD video camera, 4 microphones, and 1 ambient light sensor. It has an Intel 32 bit architecture with TPM 2.0 support and a Custom-built Microsoft Holographic Processing Unit (HPU 1.0). HoloLens uses Unity to develop applications. Unity is a cross-platform game engine developed by Unity Technologies. It uses C# as its scripting language. For detailed specifications see [16]

(a) (b)

(c)

Figure 2.4: Components of HoloLens. (a) HoloLens Display. (b) HoloLens Sensors. (c) HoloLens Motherboard. Image reproduced from [16].

2.2.1.1 User Interface

HoloLens provides multiple ways to interact with the holograms. The Mixed Reality documentation provided by Microsoft uses the 'Hologram' to define virtual objects. This term

should not be confused with actual holograms that are generated by light interference patterns. Some of the features of HoloLens that are important to our application are described below.

1. **Gaze and Gestures**: Gaze input gives the direction along which the users' head is facing. The gaze is implemented by tracking the orientation of the users head and projecting a ray in the forward direction they are facing. The gesture input captures and recognizes the users hand gestures to perform operations. HoloLens uses gaze internally to know the direction in which the user is facing and render holograms present in that direction.

   Gestures are hand patterns that are recognized by HoloLens. Currently, HoloLens recognizes two core component gestures - Air tap and Bloom (see Figure 2.5). Gaze and Gesture inputs together allow the user to interact in a natural way with the environment like gazing at an object and selecting them using air tap gestures.

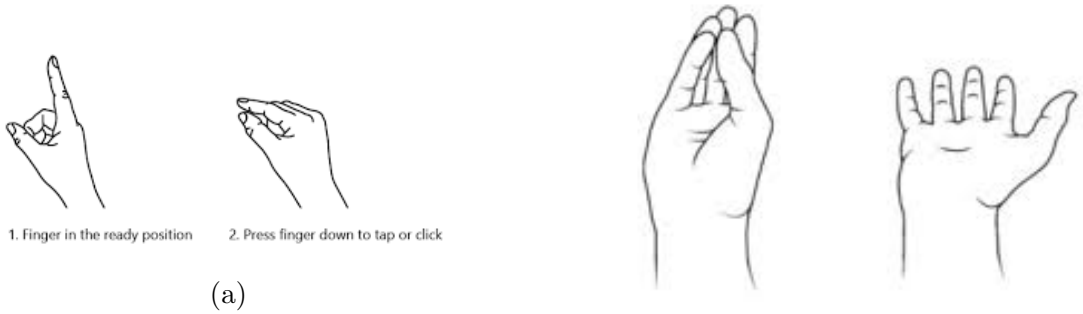

(a) (b)

Figure 2.5: Types of Gestures. (a) Air Tap (b) Bloom. Source: Microsoft Mixed Reality Docs.

2. **Voice Input**: Voice input allows the user to perform tasks just by commanding a hologram without any use of gestures. HoloLens provides voice support using keyword recognizer, grammar recognizer and dictation recognizer modules. We use the grammar recognizer module as it allows complex phrases to be detected.

3. **Spatial Mapping**: Spatial mapping provides a representation of the real world environment surrounding the HoloLens. It allows the user to have a mixed reality experience where the holograms can interact with the real world objects based on the representation formed. HoloLens performs SLAM (Simultaneous Localization and Mapping) to estimate its pose in the physical world based on its understanding of the surrounding environment. HoloLens updates the spatial mapping if it detects any changes, addition or removal of objects in its surrounding. Developers can also use the spatial mapping information in their application and provide the ability for holograms to interact with the real environment.

2.2.1.2 Hardware Characteristics

It is highly important to understand the characteristics features of any hardware in order to create robust and efficient applications. Before we get into these limitations, let us define certain terminologies to aid our understanding. The following provides a summary to the details given in [1]

2.2.1.3 Terminologies

Spatial Coordinates System : It represents the Cartesian Coordinates system used by HoloLens to position the holograms that have a real meaning in the physical world. This implies a hologram rendered 2m away from a reference frame will appear 2m away in the physical world as well. HoloLens applications, as developed by Unity, follows a left-handed coordinate system.

World Reference Frame (WRF) : HoloLens maintains a reference frame that is created by its current understanding of the physical world. It remains stationary to the physical world unless a significant change occurs in its understanding of the surrounding environment. All gameobjects/holograms and other reference frames act like a child to this world reference frame. (i.e) Any changes to the WRF will impact the position of holograms in the world. The

HoloLens creates the WRF while simultaneously localizing its position with respect to the WRF (given by the T^{H}_{WRF}). Using the location of the Hologram (given by the transformation T^{HG}_{WRF} and the localization of its pose, the HoloLens provides visualizations of the holograms with respect to the location of the user wearing the HoloLens (given by the transformation T^{HG}_{H}). Figure 2.6 shows these key frames and the transformations

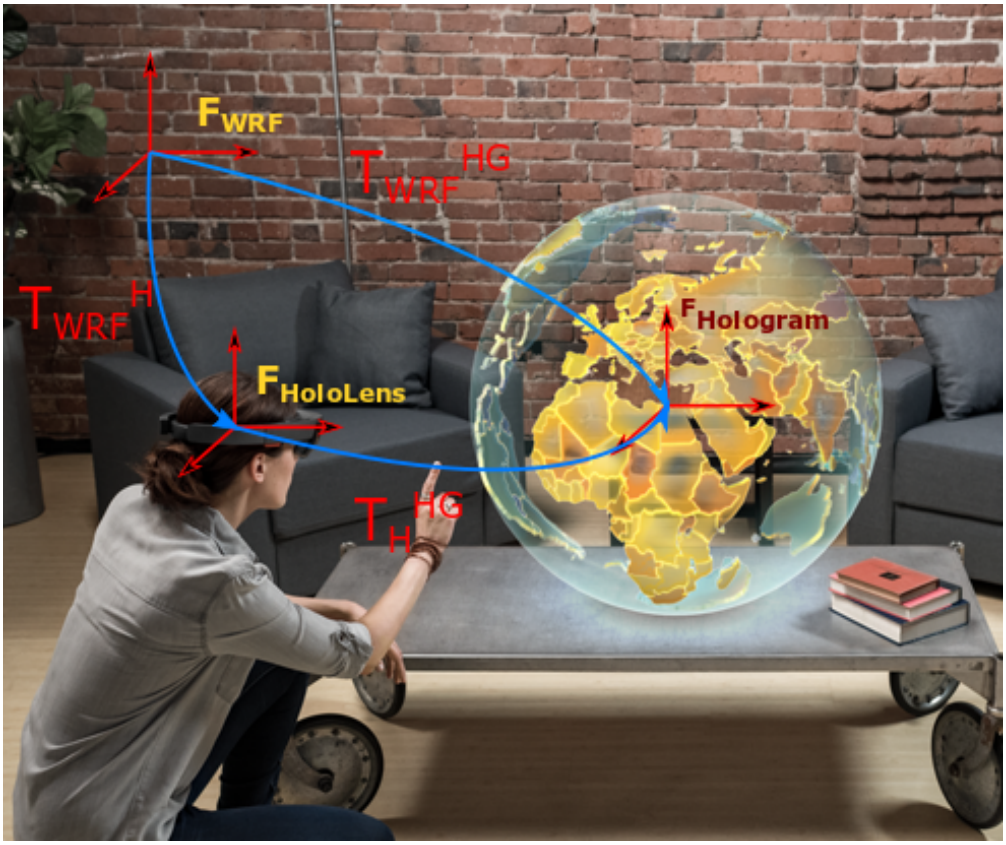

Figure 2.6: Key Frames and transformation involved between the WRF, the HoloLens and a Hologram. Image adapted and modified from Microsoft documentation

Frame Rate : Frame rate represents the number of images/frames HoloLens renders per second. The HoloLens renders images at 60 FPS (Frames Per Second).

Motion-Parallax : Motion parallax is a monocular depth cue in which we view objects that are closer to us as moving faster than objects that are further away from us.

Spatial Anchors : A spatial anchor represents an important point in the world that the system should keep track of over time. Each anchor has a coordinate system that adjusts as needed, relative to other anchors or frames of reference, in order to ensure that anchored holograms stay precisely in place. Rendering a hologram in an anchor's coordinate system gives you the most accurate positioning for that hologram at any given time. As HoloLens explores or notices changes in the environment, its understanding of the world changes and thereby the physical location of the world reference frame changes. So the system makes small adjustments to the position of anchored holograms to maintain its physical location as HoloLens updates its environment understanding.

IPD-Calibration : IPD or Interpupillary distance calibration calculates the distance between the pupils of the eyes. This distance varies from user to user and it is important to calibrate the device to each user to have a stable appearance of holograms at the right locations. HoloLens provides a calibration app that does exactly this.

Sensor Tuning : Sensor tuning denotes calibration of sensors which when not done can degrade environment mapping and lead to hologram instability.

Characteristics

1. **Head Localization**: To draw holograms such that they behave like real objects in the physical world, HoloLens needs to render images from the user's position. Since image rendering takes time, HoloLens uses a proprietary algorithm to approximate where a user's head will be when the images are shown in the displays. HoloLens has hardware that adjusts the rendered image to account for the discrepancy between the predicted head position and the actual head position. This makes the image the user sees appear as if it was rendered from the correct location, and holograms feel stable. The image updates work best with small changes, and it can't completely fix certain things in the rendered image like motion-parallax.

2. **Stabilization**: HoloLens automatically performs a sophisticated hardware-assisted holographic stabilization technique based on users motion and gaze. A single plane, called the stabilization plane, is chosen to maximize this stabilization. While all holograms in the scene receive some stabilization, holograms in the stabilization plane receive the maximum hardware stabilization. So applications should make sure that holograms reside near this plane whenever possible. Figure 2.7 show an example of stabilization plane placement. HoloLens by defaults sets the normal of the stabilization plane to be the user's gaze so that stabilization always occurs to holograms in front of the user.

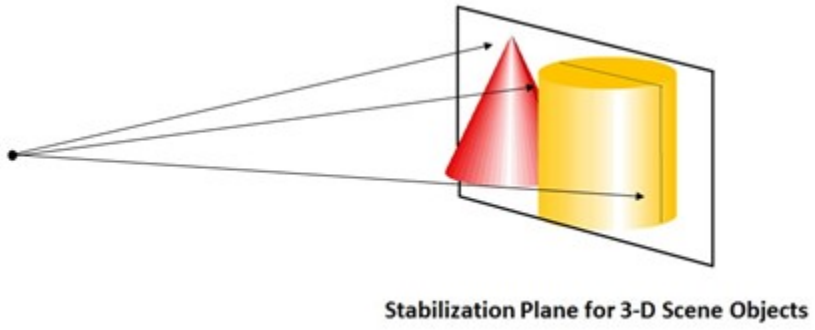

Figure 2.7: Stabilization Plane. Image reproduced from [1].

3. **Frame Rate Consistency**: Applications should make sure that they run consistently at 60 FPS for the smoother rendering of holograms. Frame rate consistency is as important as a high (60 FPS) frames-per-second. A constantly fluctuating frame rate is a lot more noticeable to a user than running consistently at lower frame rates. For example, an application that renders smoothly at 60 FPS for 5 frames and then drops to 30 FPS for the next 10 frames will appear more unstable than an application that consistently renders at 30 FPS. The maintenance of a consistent and high (60) FPS depends on a lot of factors. But one can usually narrow down the causes for inconsistency by profiling the CPU (Central Processing Unit) and GPU (Graphical Processing Unit) usage of the particular application in HoloLens. Peaking the capacity

of either of these units will result in a drop of the FPS and further analysis could be made to find the causes of the peaking

Hologram Instability

The last section gave us a solid understanding of the characteristics of the device that will be useful for our purpose. When the device is used by an application or at an environment that leads to the failure of certain characteristics, the rendered holograms become unstable. In order to develop better applications, One must also understand the instability and relate them to the appropriate characteristic failure that could have caused it. The following instability effects that we face in our application and their causes.

1. **Jitter**: Users observe this as high frequency shaking of a hologram. This can happen when tracking the environment degrades. This happens when the sensors of the HoloLens drift. The sensor tuning application provided by HoloLens should be used for this purpose.

2. **Judder**: Low rendering frequencies result in uneven motion and double images of holograms. This is especially noticeable in holograms with motion. This problem occurs when there were application tasks that consumed a lot of time to complete. Developers should make sure that the HoloLens consistently runs at 60 FPS.

3. **Drift**: Users see this as hologram appears to move away from where it was originally placed. This happens when holograms are placed far away from spatial anchors, particularly in parts of the environment that have not been fully mapped. Creating holograms close to spatial anchors lowers the likelihood of drift.

4. **Jumpiness**: When a hologram “pops” or “jumps” away from its location occasionally. This can occur as tracking adjusts holograms to match an updated understanding of the environment.

5. **Swim**: When a hologram appears to sway corresponding to the motion of the user's head. This occurs when holograms are not on the stabilization plane, and if the HoloLens is not calibrated for the current user. The user can rerun the calibration application to fix this. Developers can update the stabilization plane to further enhance stability.

Overall, With careful considerations of the above characteristics and its effects, the stability of holograms can be drastically improved. Reid Vassallo et al. [25] measured the stability of hologram's pose as disruptive actions like Walking, object insertion (updates environment understanding (spatial mapping)), sudden acceleration and occlusion (degrades tracking) were performed. They found the displacement error to be in the sub-centimeter region which is fairly accurate considering the other sources of error mentioned (human error and software calibration error) in the paper that could have potentially increased the displacement error.

2.3 Image Guided Surgery (IGS)

Figure 2.8: generic optical tracking IGS system is shown at the left and a generic EMF IGS system is shown at the right. The surgeon stands opposite a video monitor that shows the position of the tracked probe on a preoperative image such as a CT or MRI. Image reproduced from [13].

Image-guided surgery (Figure 2.8) (IGS) involves linking a preoperative image (CT, MRI, Ultrasound, etc.) to a patients intraoperative anatomy, allowing one to navigate using the image as a guide or map. A typical IGS procedure will involve a track-able surgical instrument, whose location is mapped onto this linked preoperative image and displayed on a monitor, thereby giving feedback to the surgeons on the location of their surgical tool in the operating site[13]. Figure 2.10 shows a generic setup of the IGS system. IGS improved the success rate of MIS by a great extent as endoscopic views of internal organs were often cluttered with blood and unrelated tissues that made it difficult for surgeons to know if they have reached the target location. Maria Luz et al.[15] have reviewed literature in terms of IGS impact on surgeons performance and found consistent evidence for a positive impact of IGS on patient safety and surgical outcome. In our application, we would have used a CAD model as our medical image (more details on chapter 3). But for the sake of clarity, we have summarized the IGS components as described in the literature with medical Images. The next section summarizes the book written by Robert.F.Labadie et al. [13] to give an overview of the various components involved in IGS

2.3.1 Components of Image Guided Surgery

2.3.1.1 Imaging

Imaging creates a visual representation of the interior of a body for medical intervention. Figure 2.9 shows an example of CT and MRI images take from a patient at approximately the same anatomical location.

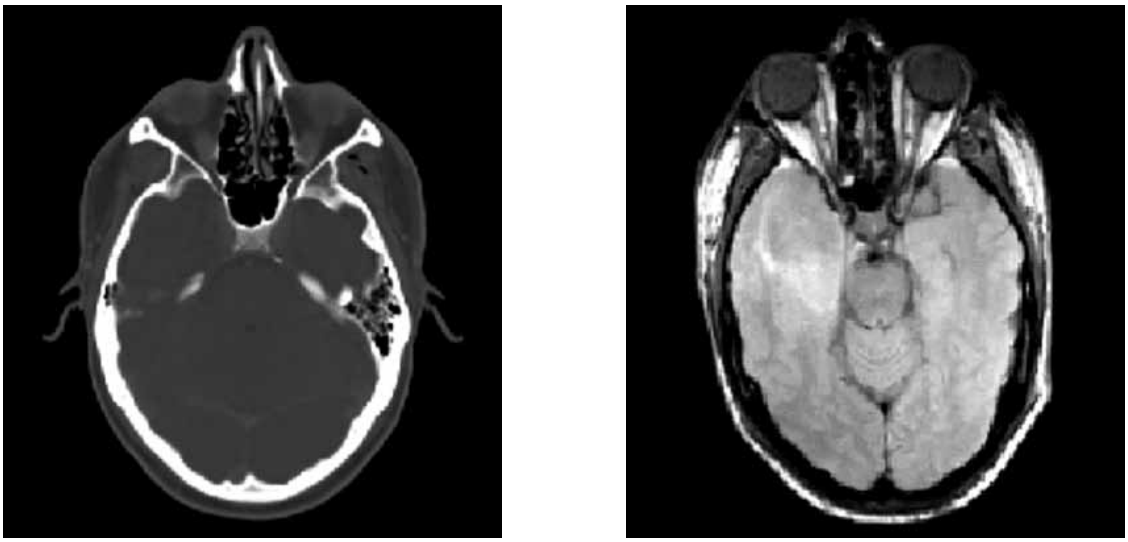

(a) (b)

Figure 2.9: Two axial images, each taken from the same patient and each at approximately the same anatomical position. **(a)** CT image,**(b)** MRI Image. Image reproduced from [13].

2.3.1.2 Tracking Systems

Now that we have our navigational Medical Images, we need the ability to detect and track the location of the surgical tools and get its location with respect to the medical images. In IGS, surgical tools also include fiducial markers that are used to track the patient location. Currently, the two most widely used tracking systems in IGS are optical tracking, that uses either visible light or infrared radiation, and electromagnetic (EM) tracking, that uses a magnetic field produced by electromagnets. Optical tracking is more accurate but it suffers from the requirement for line-of-sight (LOS). Anything that blocks this LOS temporarily disables IGS. Our application will be using an EM Tracking system as it is readily available with us and Optical tracking systems occupy larger spaces which would have been a problem to set it up in our lab. Figure 2.10 shows optical and EM tracking systems.

(a) (b)

Figure 2.10: Tracking systems: **(a)** The NDI Polaris Spectra (in back) and Vicra (in front) are the industry standards for infrared (IR) tracking **(b)** Northern Digital, Incs current commercial offering of EM tracking systems the larger Aurora planar model (shown in the back) and the smaller Aurora tabletop model (shown in the front). Image reproduced from [13].

2.3.1.3 EM Tracker

The basic concept behind EM tracking involves space and time-varying magnetic field that covers a portion of the surgical space. Surgical tools that have magnetic field sensors attached continuously measures the field at the location of the surgical tool within this portion of the surgical space. These sensors also report their measurements continuously to a system where the sensors' pose is inferred.

Our EM tracker (NDI Aurora) uses AC(Alternating Current) as its supply, which induces eddy currents when conductive materials are present in the vicinity. These materials then generate their own magnetic fields which interfere the EM field of the tracker. This is one of the main shortcomings of EM trackers as one must make sure to not have any iron/ferromagnetic materials near the device for higher tracking accuracy.

2.3.1.4 Registration

We have our Medical Images and we can also track the position of the surgical tools and fiducials. The next step is to map the position of the tools onto the medical images. Registration is the process of finding the transformations required for this mapping. In registration, the location of the fiducials on the image, are identified and aligned with the actual location

of the same fiducials on the patient measured by the EM Tracker. By aligning the fiducial's image and the actual fiducials, we will be able to align all points of interests between the image and physical space. It should be noted that from a mathematical point of view, fiducials are just points whose locations are known in both the spaces that are going to be registered. So to register two 3D spaces, we need the corresponding location of a minimum of 3 points/fiducials in each space. This registration process is performed in our application with the Principle Component Analysis (PCA) algorithm (point registration) This algorithm finds the rigid transformation between the two spaces that minimize the sum of squares of the distances between the corresponding locations of the points/fiducials.

2.3.2 Error Analysis

Just as in the case of HoloLens, the reality is always imperfect and as a result, it is critical that we understand how to minimize tracking error for given applications. The next section gives us an overview of the accuracy limitation in each step of IGS.

2.3.2.1 Accuracy Limitations

Imaging and Tracking : Accuracy of Imaging depends on the ability of the image space to localize the position of fiducials. Even though tracking is highly accurate, it can never be done perfectly. Therefore, it also has an error associated with the localization of the tools and fiducials.

Registration : The accuracy of registration can degrade due to extrinsic and intrinsic errors. The extrinsic error includes user error like the incorrect incorrect setup of the tracking system, undetected motion such as the movement of a reference frame relative to the patient. Extrinsic sources of error can be eliminated by careful use of the IGS system. Intrinsic errors, on the other hand, are errors that are generated due to localization errors in each

component of the IGS system. These errors can be estimated using statistical tools which will be discussed in the next section.

2.3.2.2 Error Measurements

Fiducial Localization Error (FLE) : The intrinsic errors made by all these systems (Imaging and tracking systems) result in the imperfect localization of fiducial points, both in the image and physical space. This imperfection is called Fiducial Localization Error (FLE).

Fiducial Registration Error (FRE) : Though FLE cannot be estimated directly, its effects can be seen during the process of registration. Error in localization will lead to an erroneous correspondence of the location of fiducial points in both the spaces, thereby leading to a bad registration. As mentioned earlier, the registration algorithm minimizes the sum of squares of the distances between the corresponding locations of the points/fiducials. This minimized value can be used as a measure to indicate the accuracy of the registration and it is proportional to the Fiducial Registration Error (FRE). (i.e) The higher the FRE, the higher will be the minimized value, the lower will be the registration accuracy and vice versa. The FRE is defined as Root Means Squared (RMS) value of the difference between the location of fiducial points in both spaces. Mathematically, It is represented as:

$$RMS\ FRE = \sqrt{\frac{1}{N}\sum_{i=1}^{N} ||p'_i - q_i||^2} \tag{2.1}$$

where,

N = No. of Fiducials,

p_i = 3D location of i^{th} fiducial in space 'p',

p'_i = Point P_i after transformation from space 'p' to space 'q',

q_i = 3D location of i^{th} fiducial in space 'q'.

Expression (2.1) shows that each term in the sum is either positive or zero, which implies that if there is at least one misalignment in the points after registration, FRE will be nonzero. Thus, a nonzero FRE proves that one or more FLEs are nonzero. Increasing the no. of fiducials will increase the FRE as it becomes more difficult for the registration algorithm to find a transformation that will bring each pair in the two spaces together.

Target Registration Error (TRE) : FRE gives us a measure of the "goodness of alignment/registration" of the fiducial's location in both the spaces. Ultimately, we would like to know an estimation of the error at a target point where we will be using our tools. This target point is usually not visible in physical space as it is usually located within the patient. This error is called Target Registration Error (TRE) and since the target is invisible, TRE is also invisible, (i.e) it can only be measured statistically. Mathematically relation between RMS TRE and RMS FRE is given in expression (2.2). This expression suggests that the RMS TRE will be minimal at the centroid of the fiducial configuration.

$$RMS\ TRE = \frac{1}{\sqrt{N-2}}\sqrt{1+\frac{d_1^2}{3f_1^2}+\frac{d_2^2}{3f_2^2}+\frac{d_3^2}{3f_3^2}} \times RMS\ FRE \tag{2.2}$$

where,

N = No. of fiducials,

d_i = Distance of the target point from one of the three "principal axes of the fiducial configuration.

f_i = RMS distance of the N fiducials from one of the principal axes.

Figure 2.11 illustrates the errors associated with registration. The image on the left shows the image space. The circles represent the actual location of the fiducials while the dots represent its measured location. The cross shows the location of the target in the image space. The difference between the dots and circle's denotes the FLE in the image space. The image on the right shows the physical space. The circles represent the actual location of the fiducials while the plus represents its measured location. The diamond shows the location of

the target in physical space. The difference between the plus and circles denotes the FLE in the physical space. The image in the center shows the registration of both the spaces. the difference between the plus and the dots represents the FRE while the difference between the cross and the diamond represents the TRE. A registration process must make sure that the TRE is minimum.

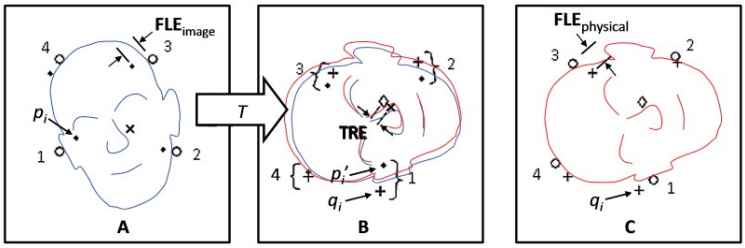

Figure 2.11: Illustration of the registration process with the associated errors. Image reproduced from [13].

This section provided a detailed picture of the working of IGS systems. We got an idea on how medical images are generated and on how the instruments are tracked and how we used both this information to perform registration. The next step will be to display this information somewhere easier for surgeons to see and understand. Once again, just as in the case of MIS, displaying this information on a monitor makes it a challenge for surgeons to perform surgical maneuvers, especially with the surgeons also requiring to look at the endoscopic view. With the advancements in computer graphics, research has been done to improve display systems by using Augmented Reality to superimpose the IGS data on to the endoscopic view thereby making the endoscopic view more intuitive[9, 17, 2]. In recent years research has been conducted looking into the possibility of using Head Mounted Devices like HoloLens to act as displays during surgical interventions. Since we will be using HoloLens for our application, in the next section, we will discuss some of the recent research that looks into the potential of HoloLens as a display for IGS.

2.4 Previous Work

Cosentino et al.[6] have developed applications for HoloLens to visualize, medical information such as navigation planning for radiotherapy, treatment procedures for educational and demonstration purposes. They have utilized the additional spatial dimension provided by HoloLens to develop intuitive visualizations. Figure 2.12 shows a visualization developed by them.

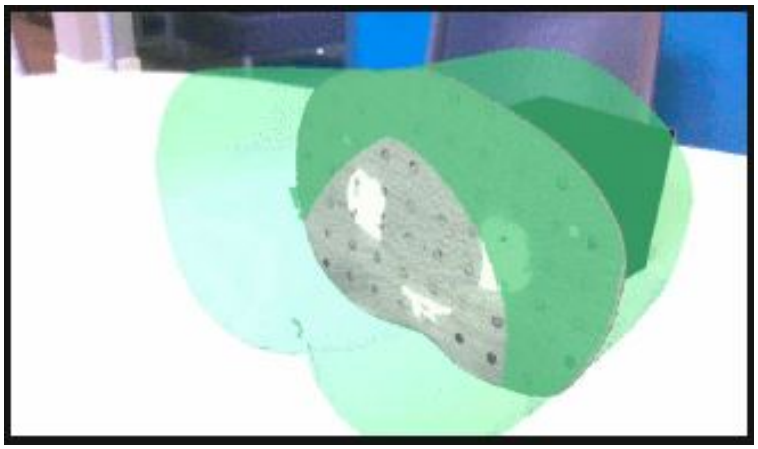

Figure 2.12: Visualization of phantom body outline and CT slice. Image reproduced from [6].

Rae et al.[23] have used HoloLens to superimpose a phantom patient's head with a hologram to mark a burrhole on the skull. They have used registration accuracy and burrhole marking time as a measure of feasibility for this setup. A rough 3 point registration was done placing virtual fiducials over the phantom and the hologram was then manually adjusted for fine registration. Registration accuracy was determined by measuring the distance between the holographic and physical markers. They have reported a clinically acceptable accuracy range of 10 mm with an average time of 4:46 mins for inexperienced users. Using 3 point registration to bring the hologram close to the site will help significantly in manual hologram placement. Since they use HoloLens only for burrhole placement, they do not have patient tracking as part of the application. Figure 2.13 show the registration process used in [23].

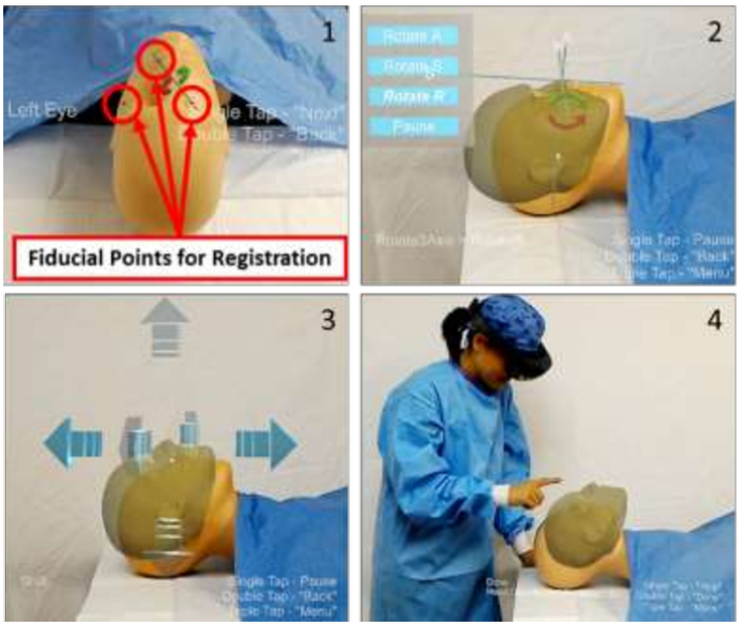

Figure 2.13: The registration process with fiducial markers (1), the tool for rotating the model (2), the tool for translating the model (3), and a view of the model in relation to the surgeon (4). Image reproduced from [23].

El-Hariri et al.[7] have proposed a method that uses tracked ultrasound intra-operatively to locate bone structures and registers them to the corresponding pre-operative computed tomography (CT) data and the generated 3D model is superimposed over the actual surgical scene using HoloLens. Vuforia (AR and image processing Software) was used for tracking a target image attached on a phantom pelvis and to place a coordinate reference frame which was used for registering the HoloLens space with the other system. The optical tracker was used for detecting the position of the ultrasound using a probe attached to the ultrasound system. Figure 2.14 shows the system setup used in [7].

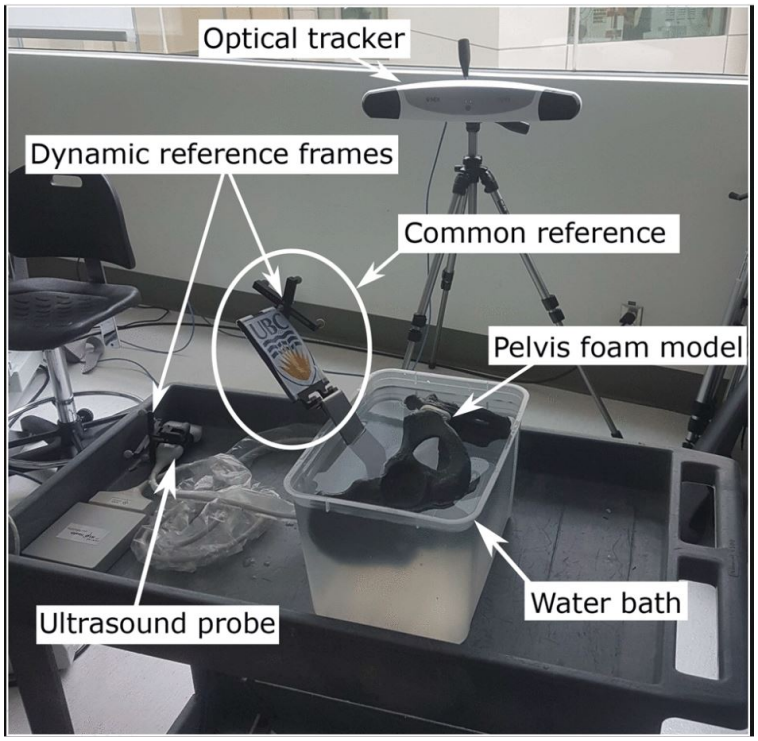

Figure 2.14: Experiment set-up showing the optical tracker, Ultrasound probe, and foam pelvis model submerged in a water bath. Image reproduced from [7].

The optical tracker also tracks the pose of a stylus that acts as a surgical tool. Figure Using a separate optical tracker avoids manual registration, therefore increasing registration accuracy. Attaching a trackable printed target to a bone can limit the scalability of this setup to clinical applications. Using plane targets for tracking using Vuforia can degrade if the user's orientation is highly oblique to the orientation of the target. The stylus is not recognized by the HoloLens which makes it difficult for the users to understand its location near a hologram. Figure 2.15 shows the final superimposition of the hologram over the actual model.

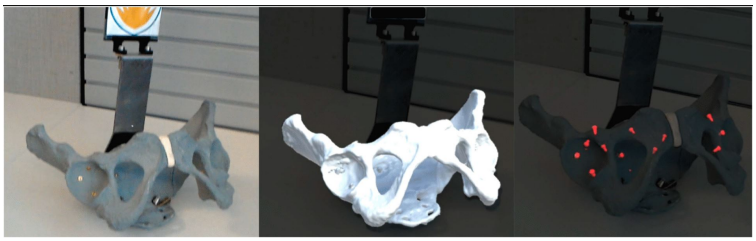

Figure 2.15: The real pelvis foam model (left), the same model with virtual pelvis overlay (middle), and the same model with virtual fiducials overlay (right). Image reproduced from [7].

Frantz et al.[8] have investigated the stability of holograms superimposed over Phantom skull anatomy when they are generated by HoloLens using Vuforia as tracking software. Cylindrical target was used for Vuforia to improve tracking stability. Registration time, Hologram drift and localization accuracy were used as metrics to study the effects of Vuforia tracking on hologram stability. They were able to demonstrate that HoloLens with Vuforias tracking provided significantly greater hologram stability than without it. Using cylindrical targets removed the problems associated with the plane target but as before, using Vuforia requires the target to be within line of sight which becomes a problem when the user is very close to the phantom model. Figure 2.16 provides tabulated results that show the superiority of Vuforia tracking with HoloLens in terms of mean perceived drift from different angles of viewing and localization accuracy.

Table 2 Change in mean perceived drift for each measurement angle

Condition	−90°	−45°	0°	+45°	+90°	Mean	σ	SEM
control, mm	6.27	3.59	0.62	4.60	6.90	4.39	3.34	1.29
vuforia, mm	0.83	1.46	1.24	0.08	3.42	1.41	1.08	0.67
Δ	−87%	−59%	0%[a]	−98%	−50%	−68%	−68%	−48%

[a]Shown to be insignificant.
σ, standard deviation.
SEM, standard error of the mean.

(a)

Table 3 Comparison of surface localisation results

Study	<2 mm	2–5 mm	5–10 mm	>10 mm
Rae *et al.* [9]	50%	0%	50%	0%
Proposed method				
Matched[a]	87%	13%	0%	0%
Control	19%	34%	40%	7%
Vuforia	53%	40%	7%	0%

(b)

Figure 2.16: **(a)** Comparison of change in mean perceived drift for each measurement angle **(b)** Comparison of surface localization results. Image reproduced from [8].

Kuzhagaliyev et al.[12] have developed a system that overcomes challenges associated with planning and guiding of the needle insertion process. They use an external tracker to track the pose of needle, ultrasound and the HoloLens headset. This data is transmitted wirelessly to HoloLens via TCP communication. Hand-eye calibration is used for finding the transformation between the tracker and HoloLens. Further calibrations are done to register the Ultrasound's pose and needle's pose in HoloLens. The needle is superimposed with a hologram. This work completely solves the line of sight problem that arises with using Vuforia. It also gives more freedom of movement for the users. Visualizing the needle will help users understand its pose irrespective of its actual visibility. The accuracy of the system is not reported making it difficult to access its findings. Figure 2.17 shows an illustration of the experimental setup used in [12].

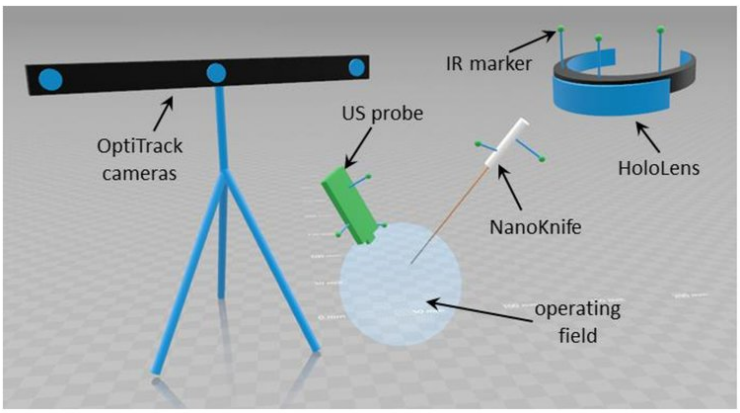

Figure 2.17: Schematic of the experimental set-up showing the relative positions of the HoloLens headset, surgical instruments and OptiTrack system components. Image reproduced from [12].

Overall, these findings give us an idea about the success of HoloLens in acting as a display for IGS in terms of registration time and accuracy. It also gives us an idea about the areas where there is a possibility for improvement. But it would also be helpful to know if this display system actually improves the ergonomics of the surgical environment. In this thesis, we will be conducting a user study to test if the ergonomics are improved and if HoloLens display would restore a surgeon's hand-eye coordination.

Chapter 3

Material and methods

The goal of this study is to find if Mixed Reality is beneficial in a navigational task during medical procedures. We will be using a simulated setup with a laparoscopy trainer model for this purpose. This chapter provides an overview of the systems and software used in this research, describing the communication workflow and the experimental setup that we used to test our hypothesis.

3.1 System Setup

Figure 3.1 shows the entire system setup. The NDI Aurora field generator is positioned vertically on a table. A custom made laparoscopic trainer model (See components Used for more details) is placed on the table within the tracking volume of the Field Generator. The reference fiducials and the probe sensor are connected to the Sensor Interface Unit (SIU). The SIU is connected to the Sensor Control Unit (SCU) which is in turn connected to the CPU of the host computer. the software was developed to extract the sensor handle name, position, orientation.

3.1.1 Components Used

The main components (Figure 3.1) involved in this setup are:

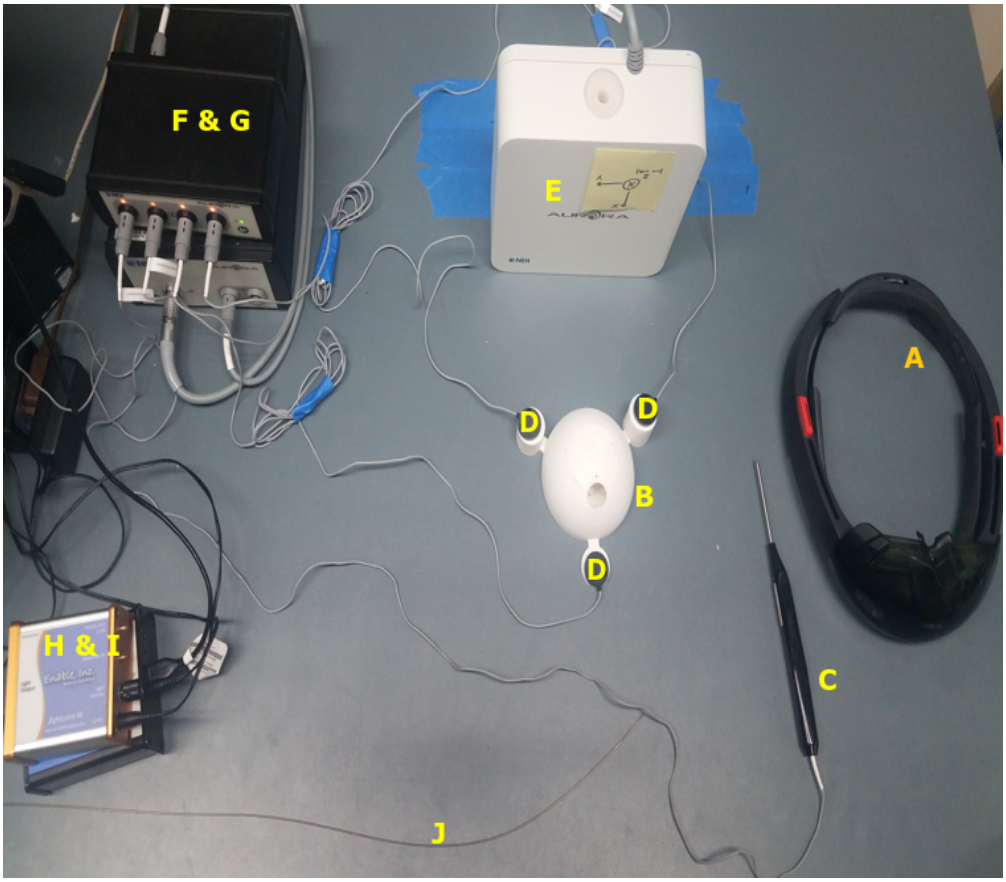

Figure 3.1: Experimental setup used in this study. **(A.)** HoloLens. **(B.)** mock laparoscopy Model. **(C.)** Sensor Probe. **(D.)** Reference Fiducials. **(E.)** Field Generator. **(F.)** SIU (Upper). **(G.)** SCU (Lower). **(H.)** lightLume-M (Upper). **(I.)** VPU-USB3-HDMI-XS (Lower). **(J.)** Endoscopic Camera.

1. **Microsoft HoloLens**: For details refer to chapter 2.

2. **NDI Aurora**: It is an Electromagnetic Tracker designed and manufactured by Northern Digital Inc. It is used in Medical fields to track surgical instruments. The following components of NDI were used in this experiment.

a) **Planar Field Generator**: A field generator emits low-intensity, varying electromagnetic field and establishes the position of the tracking volume. This experiment uses a Planar field generator that has a cubic tracking volume of 500 mm dimension and the experiments will be conducted within this volume. A track-able instrument will have a setup to generate small currents induced by the varying magnetic fields which are measured to get the location and orientation of the instrument when it is present within the tracking volume/ EM Tracker Space. Efforts should be taken to avoid any ferromagnetic material within this volume as ferromagnetic material interacts with the magnetic field and adds noise to the detection.

b) **Aurora 6DOF Reference**: It is a sensor that acts as a reference fiducial and is fixed onto the mock laparoscopy model to tracks any changes in its position and orientation.

c) **Aurora 6DOF Probe**: It is probe sensor with a rigid, straight metal tip. Subjects use this sensor to perform tasks in this experiment.

d) **Sensor Interface Unit (SIU)**: It Amplifies and digitize the electrical signals from the sensors and provide an increased distance between the System Control Unit and sensors while minimizing the potential for data noise.

e) **System Control Unit (SCU)**: It Collects information from the SIUs, calculates the position and orientation of each sensor and interfaces with the host computer. NDI provides a sample Visual Studio c++ solution (NDICombinedAPISample) to extract data from the sensors in the host computer.

3. **Endoscopic Camera**: Our experiment uses the minnieScope-XS endoscope camera designed and manufactured by Enable.Inc. We use VPU-USB3-HDMI-XS to connect the minnieScope-XS with the host computer to view the live feed on the screen. lightLume-M is used for providing lighting through the endoscope for the camera view.

4. **Mock Laparoscopy Model**: Figure 3.2 shows the custom 3D printed model designed by our lab used in this experiment. This particular design was chosen to mimic a laparoscopy trainer model with such a fiducial fixture design to reduce TRE at the center of the model. It consists of a dome that covers a base consisting of obstacles (small pin arranged in a pattern as shown in Figure 3.2). The dome has a small hole through which subjects use the probe sensor to perform tasks. An even smaller hole is present above this to provide a window for the endoscopic camera. The 3 cylinders of different heights attached to the base act as fixtures for the reference fiducials that tracks the models' position and orientation. The reference fiducials are held firmly onto the fixtures using brass threaded inserts and plastic screws instead of ferromagnetic counterparts to avoid noise in detection. This is a custom model designed and printed by our lab.

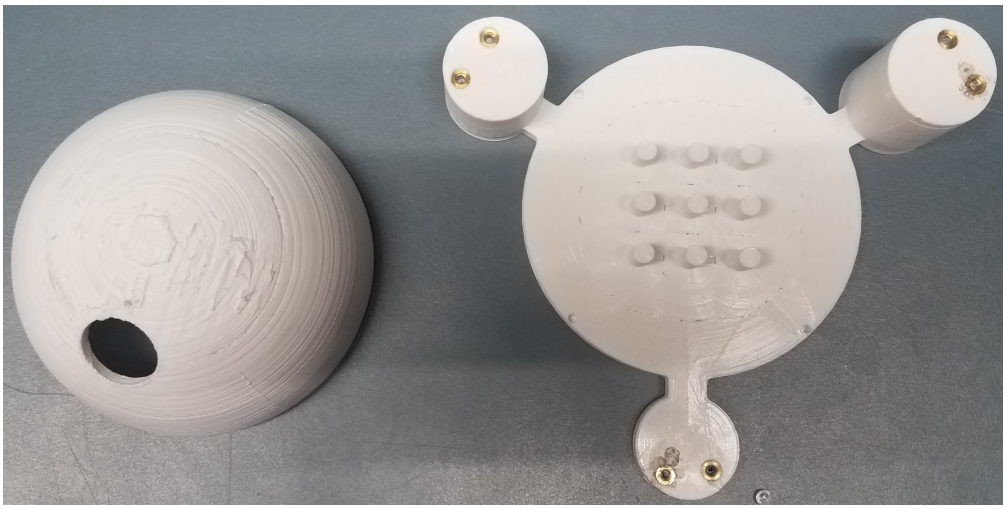

Figure 3.2: 3D printed mock laparoscopy model (dome (left) and base(right)).

3.2 Communication Work Flow

Figure 3.3 shows the data transmission flowchart between the EM Tracker to HoloLens. The movement of the probe sensor and reference fiducials from the EM Tracker is sent to the host

computer using serial communication where it is accessible via the NDICombinedSampleAPI code base. As the HoloLens in an untethered device, data transmission needs to be done through Wireless networks. Therefore, a wireless TCP connection is established between the host computer and the HoloLens. TCP or Transmission Control Protocol is a standard that defines how to initiate and manage network conversation between devices to exchange data. TCP uses a client/server model of communication where the server is the device that provides a data/resource and client is the device that requests a data/resource. In this application, The host computer acts as the server as it contains the sensor data and HoloLens act as the client and request for the sensor data from the host computer. The NDICombinedSampleAPI was slightly modified to integrate the software pipeline that makes the host computer a server capable of transmitting the sensor data upon request. Similarly, APIs were added for HoloLens to request and receive data from the server.

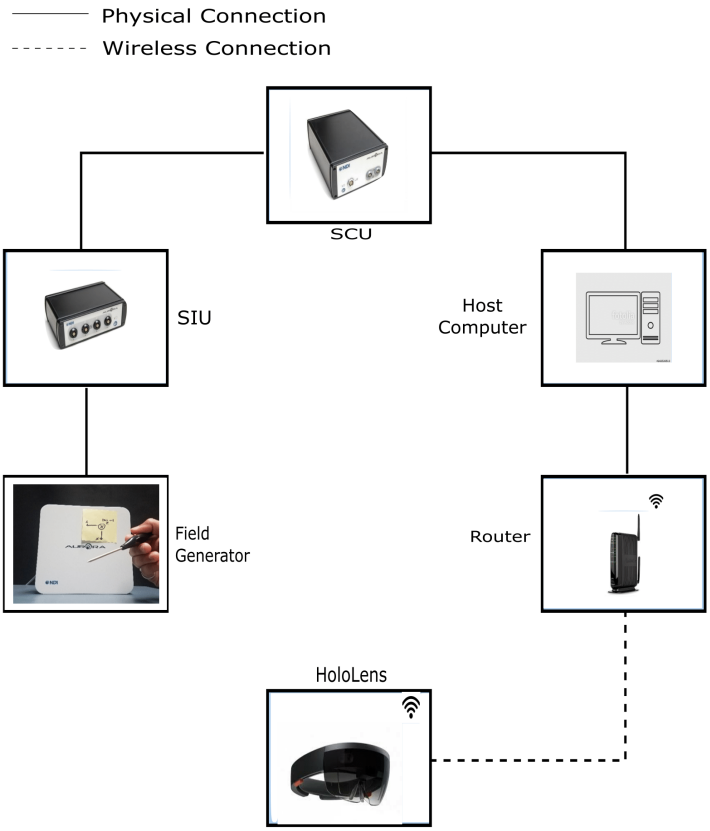

Figure 3.3: Data communication between EM Tracker and HoloLens.

3.3 Hologram - Real World registration

The goal of registration is to superimpose the hologram of the mock laparoscopy model on to the model. To achieve this, we need to find the transformations between 2 pairs of spaces. The red lines in the Figure 3.4 indicates the transformations that we need to find through registration procedures while the blue lines indicate the transformations calculated by the HoloLens based on its internal mapping and the transformations we provide.

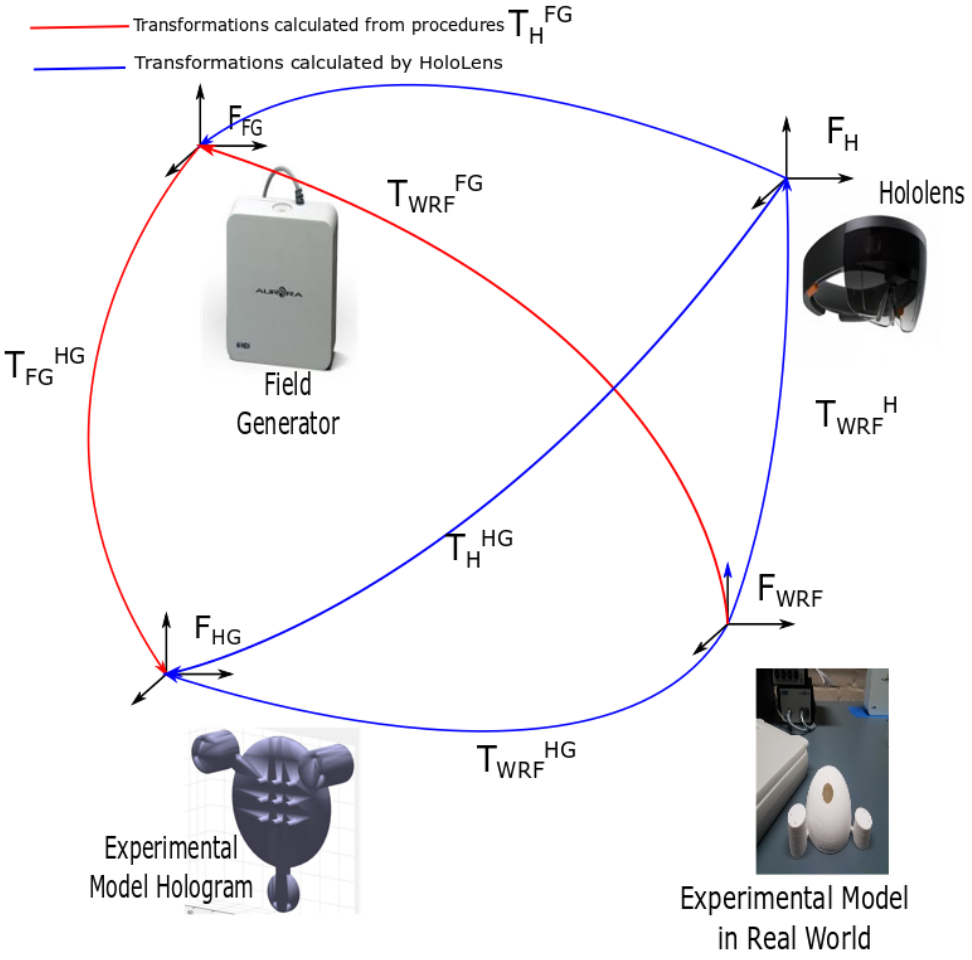

Figure 3.4: Transformations between spaces for registration.

1. **Model-EM Tracker space**: The mock laparoscopy model has 3 cylinders of different height on which reference fiducials are fixed. The fiducials are placed in such a way that the Target Registration Error (TRE) will be minimum at the center of the model. The registration tries to map the location of these fiducials measured from the origins of the EM Tracker and the mock laparoscopy model space, (i.e) it approximates the transformation between the EM Tracker and Hologram (T_{FG}^{HG}). The T_{FG}^{HG} transformation is re-calculated every frame (i.e at 60FPS) to continuously track the movements of the mock laparoscopy model.

2. **EM Tracker - WRF space**: To register these two spaces, location of fiducial points whose coordinates are known in both the spaces are required. The probe sensor is used for giving the location of any point, within the tracking volume, measured from the origin of the EM Tracker space. The World reference frame or WRF is created by the HoloLens that is stationary with respect to the world (refer chapter 2). Virtual Fiducials (Holograms) are placed within the tracking volume for giving the location of any point measured from the origin of the WRF space. Placing the probe at the center of the virtual fiducial gives the coordinates of that point in both spaces. Using multiple such points (minimum three) we can approximate the transformation between World space and the EM Tracker space (T^{FG}_{WRF}) using point registration algorithms.

The virtual fiducial is designed as a circle with a long stick of 0.5mm diameter coming out of its center to ensure the visibility of the virtual fiducial's center to the user. To ensure that the center of the virtual fiducials and the probe's tip coincide, the virtual fiducials were placed on flat surfaces with the help of planar image targets detected by Vuforia. Vuforia is an augmented reality software development kit (SDK) that enables the creation of augmented reality applications. It uses computer vision technology to recognize and track planar images (Image Targets) and simple 3D objects, such as boxes, in real time. Image targets usually require to have high contrast, intricate details, and sharp edges to have good detection. Unity provides support for Vuforia to develop applications with HoloLens. This registration is performed with the help of speech commands developed for this purpose. Figure 3.5 shows the placement of the probe over a hologram marker created by a sample image target.

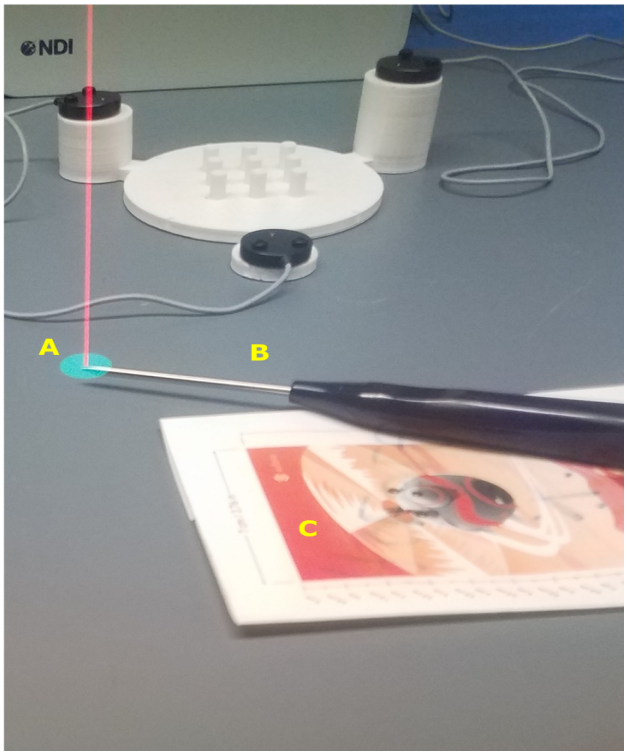

Figure 3.5: Sensor probe kept over a hologram generated by a sample image target for registration. **A.** Hologram. **B.** Sensor Probe. **C.** Sample Image Target.

The HoloLens simultaneously maps the environment and localizes its pose (SLAM) in the environment(real world). Based on the current understanding of its environment, the HoloLens creates the World Reference Frame (WRF) which act as a reference frame to the physical world (refer chapter 2). The SLAM operation gives the transformation between the HoloLens and the WRF (T^{H}_{WRF}). Using the transformations provided by us, the HoloLens calculates the transformation between the WRF and the Hologram (T^{HG}_{WRF}). This results in the superposition of the mock laparoscopy model hologram over the actual model. In order for the user wearing the HoloLens to visualize the superposition irrespective of their pose, the HoloLens uses its estimated pose to calculate the transformations between itself and the Field generator and the Holograms (T^{HG}_{H} and T^{FG}_{H}). The relation between the transformations are given as follows:

$$T_{WRF}^{HG} = T_{FG}^{HG} \cdot T_{WRF}^{FG} \tag{3.1}$$

$$T_{H}^{FG} = T_{WRF}^{FG} \cdot T_{H}^{WRF} \tag{3.2}$$

$$T_{H}^{HG} = T_{WRF}^{HG} \cdot T_{H}^{WRF} \tag{3.3}$$

Unity provides the ability to automatically calculate these transformations by allowing us to set up the parent-child relation of the gameobjects. For instance, the probe sensor is set as a child to a gameobject that represents the Field generator which in-turn is set a child of the WRF.

To avoid the mock laparoscopy model hologram drifting from their original location, We have used spatial anchors which will make sure that the location of the hologram remains intact in world space irrespective of the changes in the Spatial Coordinate system of HoloLens space. Even with all such considerations for the design and placement of virtual fiducials, placing the probe tip exactly at the center of the virtual fiducial to achieve a sub-millimeter FRE is a difficult task as it is tough to pinpoint the center of a virtual object. To overcome this problem, we have included speech commands for manual registration to fine tune the position of the hologram over the model. Figure 3.6 show the final result of the registration procedure.

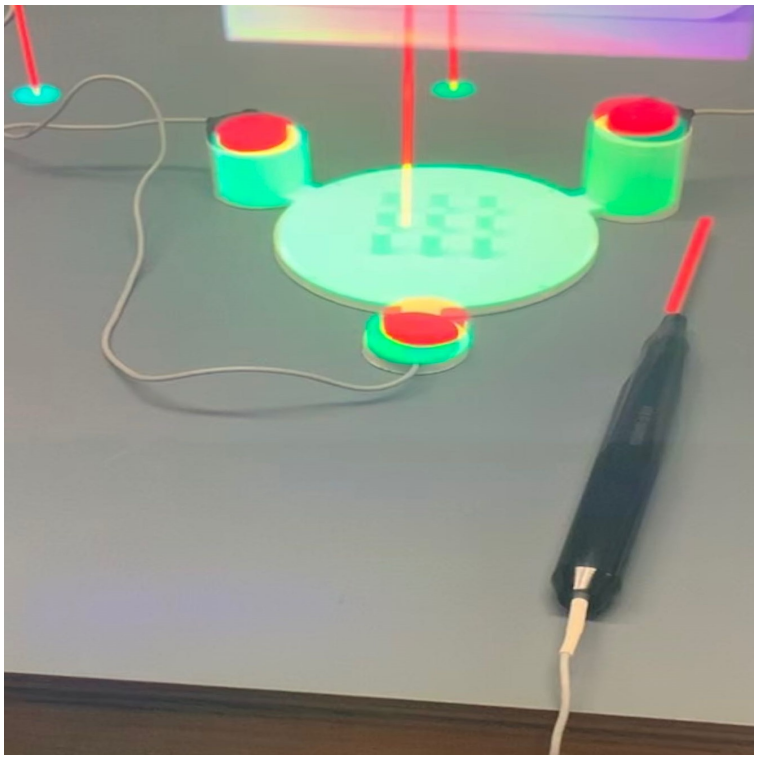

Figure 3.6: Final Registration between the hologram and the real world. This image was taken using a phone behind the display.

3.4 The Experimental Work Flow

The goal of this experiment is to understand if Mixed Reality can enhance a surgeons' performance in MIS. This Section details the experiment that is used for this purpose.

3.4.1 Study Protocol

The experiment involves human participants to perform a simple manipulation task involving tracing a prescribed path using a mock surgical instrument (Probe Sensor). This task is performed twice by the Study participants (once for each of the experimental conditions described below). During each experiment, the instrument movements are recorded through

an electromagnetic tracker (Fig. 2) along with the time required to complete the task. This experiment is approved by the Institutional Review Board (IRB).

3.4.1.1 The Task

The task involves using the sensor probe to touch the pins present in the base in a specific pattern (the task pattern). Figure 3.7 shows examples of such patterns used in the experiment. The dome encloses the base and the users can touch the pins only through the small opening provided on the dome. The task is chosen such that it is simple for users with no surgical experience to understand and perform. The movement of the probe is recorded throughout the completion of the task, which is used for calculating the time taken to complete the task (task time) and the length of the path covered by the user. No user will receive the same pattern for both the experimental conditions. This prevents prior knowledge from interfering the performance of the user.

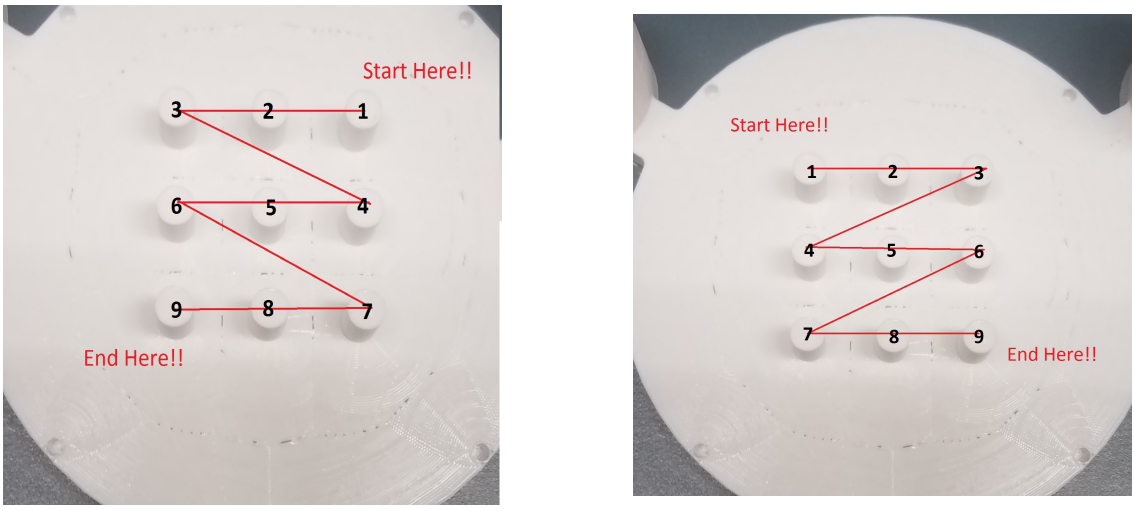

(a) (b)

Figure 3.7: Sample Task patterns used for the experiment. The red line indicates the path that needs to be traversed during the experiment. The numbers indicate the sequence in which the pins must be touched along the path.

1. **Experimental Condition 1**: In this scenario, the users perform the task while vi-

sualizing the motion of their instrument through a monitor (just like it happens in actual minimally-invasive procedures); the monitor displays a live camera feed that mimics the view of an endoscopic camera. A total of five trial runs is performed to give participants a chance to familiarize with the set-up. Figure 3.8 shows us a user performing the experiment for this condition. This experimental condition is called the Endoscope experiment.

Figure 3.8: User performing experiment with endoscopic view of the task arena.

2. **Experimental Condition 2**: In this scenario, users perform the manipulation task while wearing a head-mounted Mixed Reality display (Microsoft HoloLens, Microsoft Corp., Redmond, WA) which projects the movements of the instrument through a hologram. A total of five trial runs is performed to give them a chance to familiarize with the set-up. Figure 3.9 shows us a user performing the experiment for this condition. This experimental condition is called the HoloLens experiment.

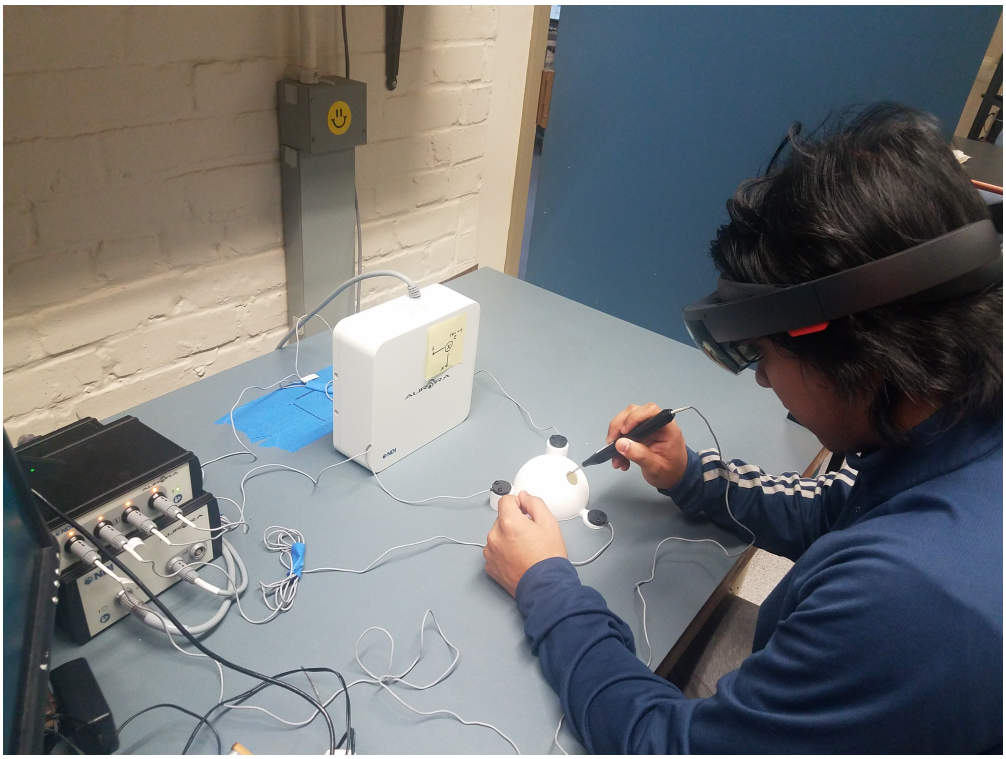

Figure 3.9: User performing experiment with superimposed view of the task arena.

The sequence in which users will complete the experimental conditions listed above will be randomized, and a resting period of one week will be observed between the two trials.

Chapter 4

Experimental Results

4.1 Results

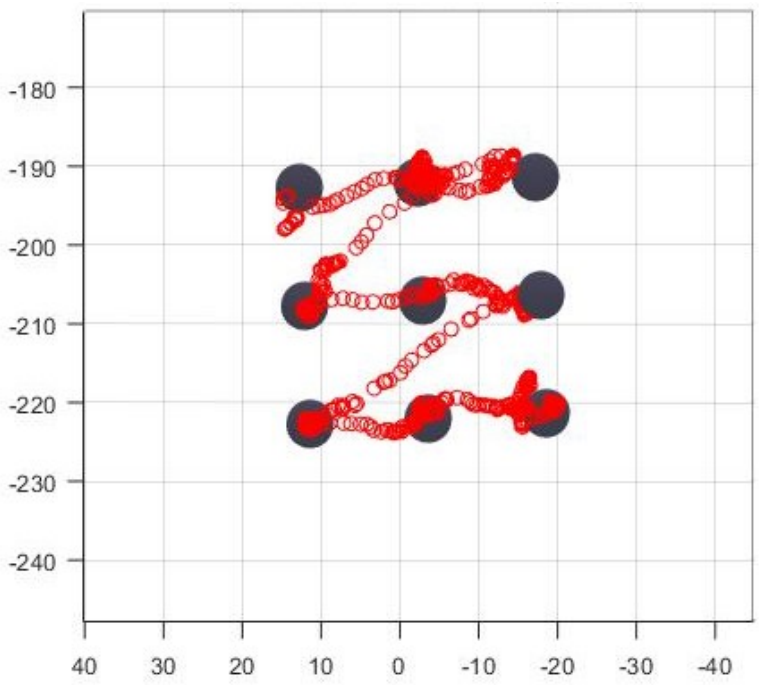

Figure 4.1: Recorded path movement of a user in performing a task for one of the experimental condition. The red circles indicate the path taken by the user while the black circles depicts the location of the pins

Figure 4.1 shows an example of the path taken by a user in completing the task for the HoloLens experiment. Five users were recruited to perform this experiment. Two simple task patterns 3.7 were used in the experiment. The correspondence of the tasks to the experimental conditions was randomized for each user. This was done to prevent the task pattern from impacting the results. The users were asked to signal during the start and end of the task to record the probe movements within that time interval. This data was used to calculate the path length and time taken (task time) for each user to complete the task in both the experimental condition. These metrics are the common ones used in surgical skill evaluation [20, 11].

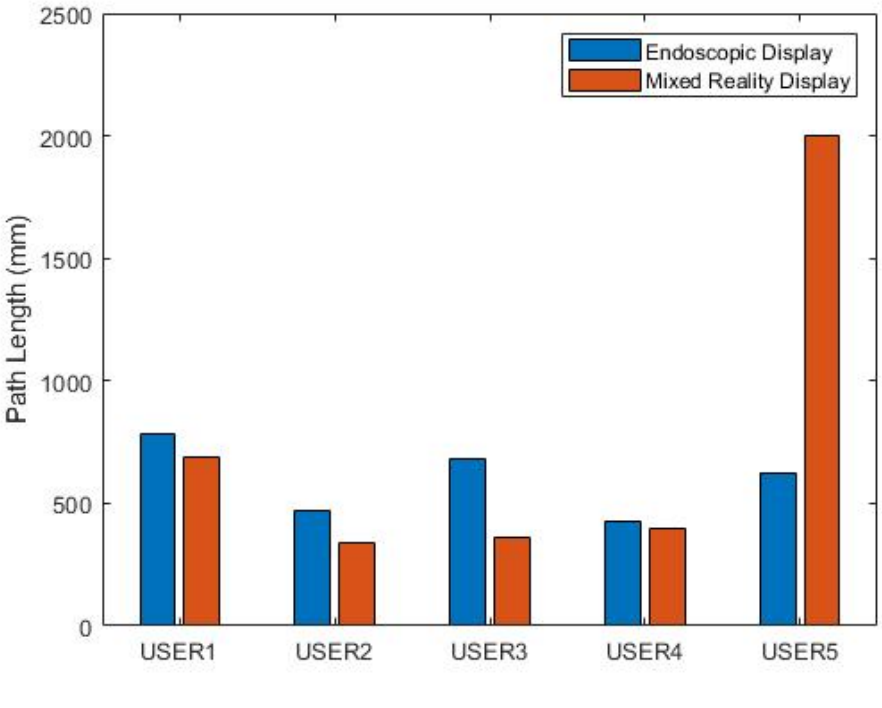

Figure 4.2: Comparison of path length for the 5 users between the two experimental conditions.

The task time is a proxy for overall efficiency while the Path length measures movement economy. Both the metrics relate inversely to the performance of our experimental

conditions. i.e lower values of the metrics imply a better performance for that particular experimental condition and vice versa. Figures 4.3 and 4.2 show that four out of five users performing the HoloLens experiment were able to finish the task faster with smaller path length and the fifth user performed better on both the metrics for the Endoscopic experiment.

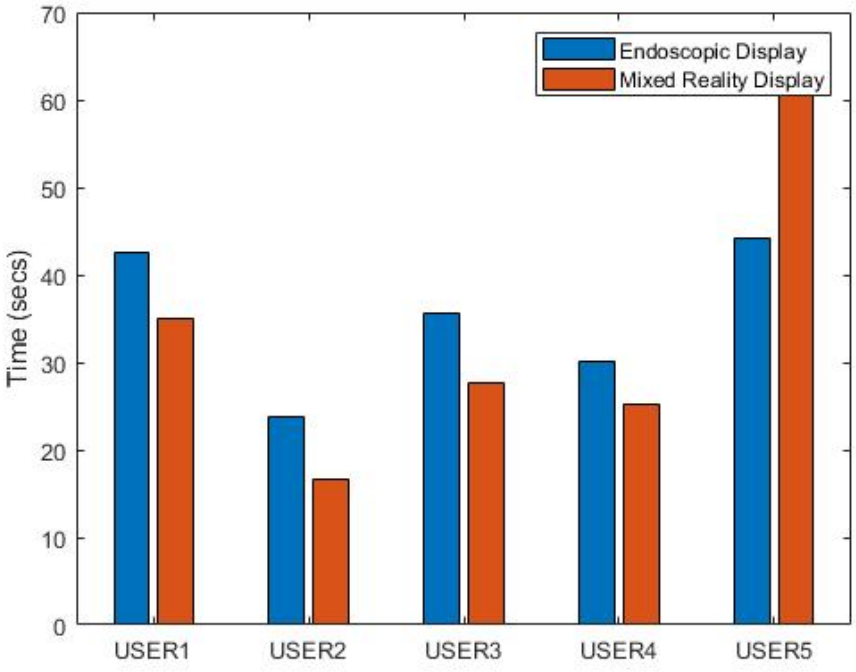

Figure 4.3: Comparison of task time for the 5 users between the two experimental conditions.

To quantitatively evaluate the performance of users in both the conditions, we define a quantity called the Percentage Difference(PD). For the given two experimental conditions, the Percentage Difference is defined as the difference in a performance metric of the experimental conditions taken as a percentage of the metric value in the endoscopic experiment. Mathematically it is given as,

$$PD = \frac{M_{E_{en}} - M_{E_h}}{M_{E_{en}}} \times 100 \tag{4.1}$$

where,

M = metric used for evaluation,

E_{en} = Endoscopic Experiment,

E_h = HoloLens Experiment.

Due to the inverse relation of our metrics to the performance, positive values of PD implies that users performed better in HoloLens experiment and negative values imply that users performed better in the endoscopic experiment. The absolute values of the PD give us a direct estimate of how well the user performed in one experiment compared to the other.

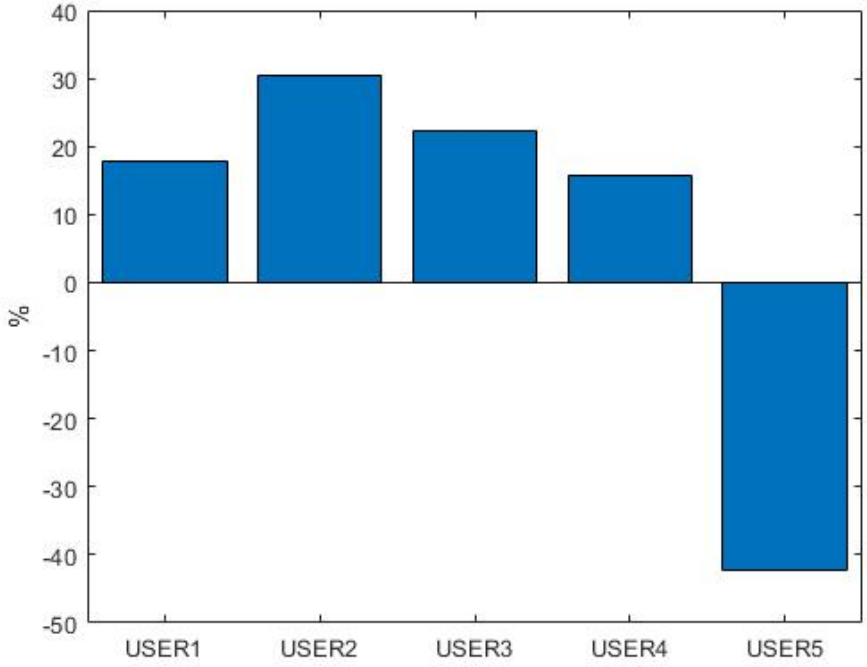

Figure 4.4: Difference of task time between the experimental conditions for each user as a percentage of the task time for the endoscopic experiment.

Figures 4.4 and 4.5 show the PD for our experimental conditions (endoscope and HoloLens) with the task time and path length metrics. The graph shows the disparity between users

who performed better with HoloLens experiment (average of 21.5% for task time and 23.9% for path length) and the fifth user who performed better in the endoscopic experiment (-42.23% for task time and -219.8% for path length).

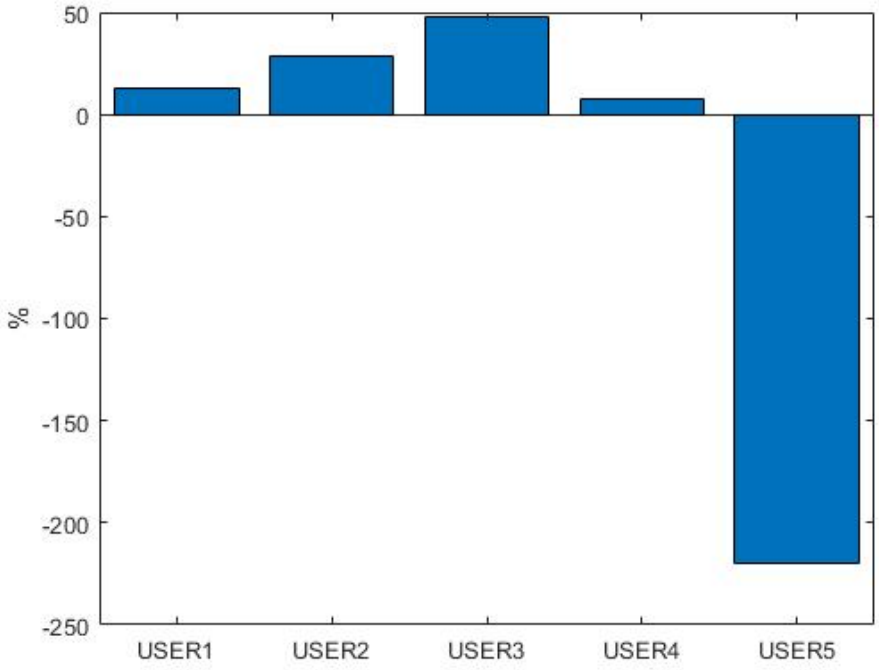

Figure 4.5: The difference of path length between the experimental conditions for each user as a percentage of the path length for the endoscopic experiment.

4.2 Discussions

The absolute PD values for the users who performed better in the HoloLens experiment are small but constitutes the average of four users while the absolute PD value for the user who performed better in the endoscopic experiment is high but constitutes only one user. With a small sample size, it is difficult to come to a conclusion in such a scenario. However, the feedback was taken from each user as part of the preliminary testing of the experimental setup. The fifth user found it difficult to differentiate the pins from the base of the hologram

and also had problems with light reflecting off of the white surface of the mock laparoscopy model which hindered the visibility of the hologram. Figure 4.6 shows the path taken by this user to complete the task with HoloLens. As one can see, the user was not able to pinpoint the location of the pins. This suggests that when the users do not face the contrast problem, they were able to perform better in the HoloLens experiment which implies that the HoloLens Experiment has a better performance than the Endoscopic experiment. A larger study with an improved system would corroborate these findings.

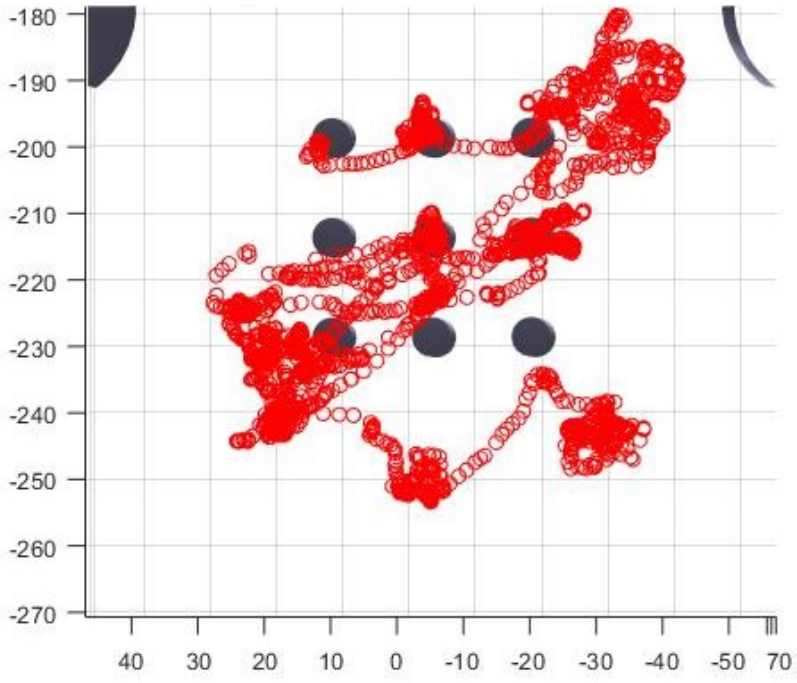

Figure 4.6: Recorded path movement of the 5th user in performing a task for the experimental condition with HoloLens. The user clearly was not able to find the pins.

4.3 Conclusions and Future Work

In this study, we developed a path following task to study the effects of using Mixed Reality on the performance of surgeons for Minimally Invasive Surgeries. Preliminary test results suggest an improvement in performance and warrants for a larger study. Before conducting

any further studies, the contrast problem will be solved by differentiating the color of the pins from that of the base. In the current study, the data transmission between HoloLens and host computer takes place via a TCP communication protocol which is not suitable for real-time communication and causes lag. This lag is not quantified as a part of this study which can be done before conducting the larger study. Also, using the UDP communication protocol for data transfer is a possible step that can be taken to improve the study. Finally, more complicated tasks can be included in the study to understand the effects of task complexity over the performance of the users in both the experimental conditions. The Mixed Reality Image Guided System developed as part of this project will be used in future studies to explore the registration process from an engineering point of view (i.e Engineering considerations to be taken in reducing TRE and FRE for this system).

Bibliography

[1] Matt Zeller Eliot Cowley Brandon Bray Alex Turner, Troy Ferrell. Hologram stability, March 2018. [Online; posted 20-March-2018].

[2] Sylvain Bernhardt, Stéphane A Nicolau, Luc Soler, and Christophe Doignon. The status of augmented reality in laparoscopic surgery as of 2016. *Medical image analysis*, 37:66–90, 2017.

[3] Nick Schonning Matt Zeller Brandon Bray, Jesse McCulloch. What is mixed reality?, March 2018. [Online; posted 20-March-2018].

[4] Alex Cameron. The application of holographic optical waveguide technology to the q-sight family of helmet-mounted displays. In *Head-and Helmet-Mounted Displays XIV: Design and Applications*, volume 7326, page 73260H. International Society for Optics and Photonics, 2009.

[5] Sara Condino, Giuseppe Turini, Paolo D Parchi, Rosanna M Viglialoro, Nicola Piolanti, Marco Gesi, Mauro Ferrari, and Vincenzo Ferrari. How to build a patient-specific hybrid simulator for orthopaedic open surgery: Benefits and limits of mixed-reality using the microsoft hololens. *Journal of Healthcare Engineering*, 2018, 2018.

[6] Francesco Cosentino. Exploration and implementation of augmented reality for external beam radiotherapy. 2018.

[7] Houssam El-Hariri, Prashant Pandey, Antony J Hodgson, and Rafeef Garbi. Augmented reality visualisation for orthopaedic surgical guidance with pre-and intra-operative multimodal image data fusion. *Healthcare Technology Letters*, 5(5):189–193, 2018.

[8] Taylor Frantz, Bart Jansen, Johnny Duerinck, and Jef Vandemeulebroucke. Augmenting microsoft's hololens with vuforia tracking for neuronavigation. *Healthcare technology letters*, 5(5):221–225, 2018.

[9] Jacob T Gibby, Samuel A Swenson, Steve Cvetko, Raj Rao, and Ramin Javan. Head-mounted display augmented reality to guide pedicle screw placement utilizing computed tomography. *International journal of computer assisted radiology and surgery*, 14(3):525–535, 2019.

[10] B Jaffray. Minimally invasive surgery. *Archives of disease in childhood*, 90(5):537–542, 2005.

[11] Timothy N Judkins, Dmitry Oleynikov, and Nick Stergiou. Objective evaluation of expert and novice performance during robotic surgical training tasks. *Surgical endoscopy*, 23(3):590, 2009.

[12] Timur Kuzhagaliyev, Neil T Clancy, Mirek Janatka, Kevin Tchaka, Francisco Vasconcelos, Matthew J Clarkson, Kurinchi Gurusamy, David J Hawkes, Brian Davidson, and Danail Stoyanov. Augmented reality needle ablation guidance tool for irreversible electroporation in the pancreas. In *Medical Imaging 2018: Image-Guided Procedures, Robotic Interventions, and Modeling*, volume 10576, page 1057613. International Society for Optics and Photonics, 2018.

[13] Fitzpatrick J Michael Labadie Robert F. *Image-guided surgery: fundamentals and clinical applications in otolaryngology.* Plural Publishing, 2016.

[14] Yang Liu, Haiwei Dong, Longyu Zhang, and Abdulmotaleb El Saddik. Technical evaluation of hololens for multimedia: a first look. *IEEE MultiMedia*, 25(4):8–18, 2018.

[15] Maria Luz, Gero Strauss, and Dietrich Manzey. Impact of image-guided surgery on surgeons' performance: a literature review. *International Journal of Human Factors and Ergonomics*, 4(3-4):229–263, 2016.

[16] Grbury Brandon Bray Matt Zeller, Alex Turner. Hololens (1st gen) hardware details, March 2018. [Online; posted 20-March-2018].

[17] Antonio Meola, Fabrizio Cutolo, Marina Carbone, Federico Cagnazzo, Mauro Ferrari, and Vincenzo Ferrari. Augmented reality in neurosurgery: a systematic review. *Neurosurgical review*, 40(4):537–548, 2017.

[18] Jene W Meulstee, Johan Nijsink, Ruud Schreurs, Luc M Verhamme, Tong Xi, Hans HK Delye, Wilfred A Borstlap, and Thomas JJ Maal. Toward holographic-guided surgery. *Surgical innovation*, 26(1):86–94, 2019.

[19] Paul Milgram and Fumio Kishino. A taxonomy of mixed reality visual displays. *IEICE TRANSACTIONS on Information and Systems*, 77(12):1321–1329, 1994.

[20] Ilana Nisky, Yuhang Che, Zhan Fan Quek, Matthew Weber, Michael H Hsieh, and Allison M Okamura. Teleoperated versus open needle driving: Kinematic analysis of experienced surgeons and novice users. In *2015 IEEE International Conference on Robotics and Automation (ICRA)*, pages 5371–5377. IEEE, 2015.

[21] Philip Pratt, Matthew Ives, Graham Lawton, Jonathan Simmons, Nasko Radev, Liana Spyropoulou, and Dimitri Amiras. Through the hololens looking glass: augmented reality for extremity reconstruction surgery using 3d vascular models with perforating vessels. *European radiology experimental*, 2(1):2, 2018.

[22] Long Qian, Alexander Barthel, Alex Johnson, Greg Osgood, Peter Kazanzides, Nassir Navab, and Bernhard Fuerst. Comparison of optical see-through head-mounted displays for surgical interventions with object-anchored 2d-display. *International journal of computer assisted radiology and surgery*, 12(6):901–910, 2017.

[23] Emily Rae, Andras Lasso, Matthew S Holden, Evelyn Morin, Ron Levy, and Gabor Fichtinger. Neurosurgical burr hole placement using the microsoft hololens. In *Medical Imaging 2018: Image-Guided Procedures, Robotic Interventions, and Modeling*, volume 10576, page 105760T. International Society for Optics and Photonics, 2018.

[24] Morgan K Richards, Jarod P McAteer, F Thurston Drake, Adam B Goldin, Saurabh Khandelwal, and Kenneth W Gow. A national review of the frequency of minimally invasive surgery among general surgery residents: assessment of acgme case logs during 2 decades of general surgery resident training. *JAMA surgery*, 150(2):169–172, 2015.

[25] Reid Vassallo, Adam Rankin, Elvis CS Chen, and Terry M Peters. Hologram stability evaluation for microsoft hololens. In *Medical Imaging 2017: Image Perception, Observer Performance, and Technology Assessment*, volume 10136, page 1013614. International Society for Optics and Photonics, 2017.